

Thermal versus Photochemical Reductive Elimination of Aryl Chlorides from NHC–Gold Complexes

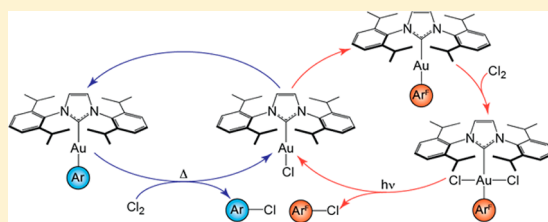
Michael J. Ghidui,[†] Allen J. Pistner,[†] Glenn P. A. Yap,[†] Daniel A. Lutterman,[‡] and Joel Rosenthal^{*,†}

[†]Department of Chemistry and Biochemistry, University of Delaware, Newark, Delaware 19716, United States

[‡]Chemical Sciences Division, Oak Ridge National Laboratory, Oak Ridge, Tennessee 37831, United States

Supporting Information

ABSTRACT: Two homologous complexes of the type [(NHC)Au^I–Ar], in which the aryl substituent was either phenyl or pentafluorophenyl, were prepared. Treatment of [(IPr)Au^IC₆F₅] with PhICl₂ leads directly to the expected Au^{III} oxidation addition product [(IPr)Au^{III}(Cl)₂C₆F₅]. This complex is thermally stable but undergoes photochemical reductive elimination to deliver [(IPr)Au^ICl] and C₆F₅Cl. In contrast, the reaction of [(IPr)Au^IPh] with PhICl₂ does not deliver an isolable Au^{III} oxidation addition product but rather leads directly to the formation of [(IPr)Au^ICl] and PhCl, presumably via a [(IPr)Au^{III}(Cl)₂Ph] intermediate. These related reactivity pathways are rationalized on the basis of the electronic structures of the two [(NHC)Au^I–Ar] complexes.



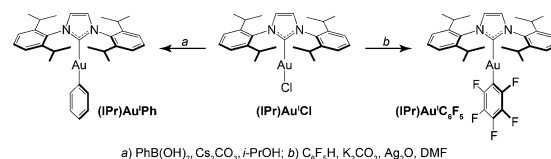
N-heterocyclic carbene (NHC) complexes of gold have found utility for the catalytic formation of C–C,^{1–3} C–O, and C–N bonds.⁴ Additional emphasis has been placed on use of such complexes for C–X (X = halogen) bond formation.^{5–7} Moreover, recent work has shown that photoexcitation of complexes of the type [(L)Au^{III}(X)₃] (L = phosphine, NHC; X = Cl, Br) leads to reductive elimination of X₂.^{8,9} Despite the recent synthetic and catalytic advances involving Au^I and Au^{III} complexes supported by NHC ligands, the ability of such systems to mediate the reductive elimination of aryl chlorides has not been demonstrated. Although previous studies have shown that other certain Cu^{10–12} and Pd¹³ complexes can promote aryl halide formation, the photochemical and/or thermal elimination of Ar–X bonds from Au^{III} complexes of the type [(NHC)Au^{III}(X)₂Ar] (Ar = aryl; X = halogen) has not been documented. To this end, we sought to probe the reactivity of [(NHC)Au^I–Ar] complexes with Cl₂, particularly with respect to thermal and photochemical elimination of Ar–Cl from the Au center.

In developing suitable platforms to investigate the reactivity described above, we adopted an NHC ligand sporting ancillary 2,6-diisopropylphenyl groups (IPr = 1,3-bis(2,6-diisopropylphenyl)imidazole-2-ylidene). The bulky aryl groups appended to this carbene ligand offer enhanced steric protection to the metal center and help to solubilize the metal complex.¹⁴ Moreover, IPr has been shown to support many interesting organometallic complexes of gold.^{15,16} In surveying the chemistry described in the preceding paragraph, we targeted two electronically distinct [(IPr)Au^I–Ar] complexes in which the aryl group was either phenyl or pentafluorophenyl.

[(IPr)Au^ICl]¹⁷ was converted to the corresponding phenyl derivative [(IPr)Au^IPh] in 66% yield via treatment with PhB(OH)₂ and Cs₂CO₃ in isopropyl alcohol at 55 °C (Scheme

1).^{18,19} The corresponding pentafluorophenyl homologue was prepared by adapting an arene C–H activation strategy that has

Scheme 1. Synthesis of (IPr)Au^I–Ar Complexes



been utilized for Au^I–phosphine complexes.²⁰ As such, the reaction of [(IPr)Au^ICl], pentafluorobenzene, and Ag₂O in DMF at 55 °C delivered [(IPr)Au^IC₆F₅] in 64% yield. Crystals of this complex were grown from CH₂Cl₂/pentane solutions via slow evaporation. The solid-state structure of this compound (Figure 1a) revealed that the pentafluorophenyl ring is canted by 75.8° with respect to the imidazole ring that comprises the IPr framework. This angle is similar to that observed for the corresponding phenyl derivative [(IPr)Au^IPh], in which the torsional angle is 88.6°.²¹ Other selected bonding metrics are given in Table 1. Notably, the Au^I–C(IPr) and Au^I–C(Ar) bond lengths of [(IPr)Au^IC₆F₅] are 2.018 and 2.021 Å, respectively. As shown in Table 1, these metrics are slightly shorter than the analogous bond lengths for the corresponding nonfluorinated complex [(IPr)Au^IPh].²¹

With both of the aryl-appended NHC–Au^I complexes in hand, we investigated the oxidation of these systems. Treatment of a CHCl₃ solution of [(IPr)Au^IC₆F₅] at 45 °C with iodobenzene dichloride (PhICl₂),²² which is a convenient source of Cl₂,²³ leads to the clean formation of a new complex

Received: July 17, 2013

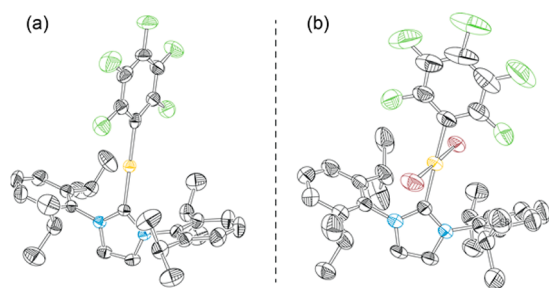


Figure 1. Solid-state structures of (a) $[(\text{IPr})\text{Au}^{\text{I}}\text{C}_6\text{F}_5]$ and (b) $[(\text{IPr})\text{Au}^{\text{III}}(\text{Cl})_2\text{C}_6\text{F}_5]$. Thermal ellipsoids are shown at the 50% probability level (F, green; Au, orange; C, black; N, blue; Cl, maroon). Hydrogen atoms are omitted for clarity.

within 3 h. The ^1H NMR spectrum obtained for this new product is consistent with oxidation of the Au^{I} complex to the corresponding Au^{III} dihalide, on the basis of the downfield shift of the ligand methyne ^1H NMR resonances from δ 2.61 to 2.90 ppm. Although only two other $\text{NHC}-\text{Au}^{\text{III}}$ complexes of the type $[(\text{NHC})\text{Au}^{\text{III}}(\text{Cl})_2\text{Ar}]$ are known,²⁴ several related complexes of this type supported by phosphine and arsine ligands have been reported.^{25,26}

X-ray diffraction studies confirmed that this material was the square-planar oxidative addition product $[(\text{IPr})\text{Au}^{\text{III}}(\text{Cl})_2\text{C}_6\text{F}_5]$. As shown in Figure 1b, the NHC and aryl ligands of $[(\text{IPr})\text{Au}^{\text{III}}(\text{Cl})_2\text{C}_6\text{F}_5]$ maintain their *trans* orientation, with respect to one another. Unlike the case for the Au^{I} precursor, however, these two ligands are only canted by 14.2° with respect to one another. Additional bonding metrics for this complex are provided in Table 1. Interestingly, the $\text{Au}^{\text{III}}-\text{C}(\text{IPr})$ and $\text{Au}^{\text{III}}-\text{C}(\text{Ar})$ bonds of $[(\text{IPr})\text{Au}^{\text{III}}(\text{Cl})_2\text{C}_6\text{F}_5]$ (2.062 and 2.049 Å, respectively) are longer than the corresponding metrics for $[(\text{IPr})\text{Au}^{\text{I}}\text{C}_6\text{F}_5]$. A similar trend has been observed for the homologous mesityl-appended $\text{NHC}-\text{Au}^{\text{I/III}}$ complexes.²⁴

$[(\text{IPr})\text{Au}^{\text{III}}(\text{Cl})_2\text{C}_6\text{F}_5]$ is stable for at least several months when stored at room temperature in the absence of light; however, we found that samples of this compound exposed to room light decomposed over the course of weeks to generate $[(\text{IPr})\text{Au}^{\text{I}}\text{Cl}]$. This observation suggested that photoexcitation of this Au^{III} dichloride complex induces reductive elimination of 1 equiv of aryl chloride. To further probe this process, solutions of $[(\text{IPr})\text{Au}^{\text{III}}(\text{Cl})_2\text{C}_6\text{F}_5]$ in CHCl_3 were irradiated ($\lambda_{\text{exc}} \geq 275$ nm) and the course of the photoreaction was monitored by ^1H NMR and UV-vis spectroscopy.

A time course for the changes in the absorption profile accompanying this photoreaction is displayed in Figure 2. An isosbestic point is maintained at 265 nm throughout the photolysis, attesting to a clean and quantitative process. The final absorbance spectrum is identical with that of $[(\text{IPr})\text{Au}^{\text{I}}\text{Cl}]$ and does not change upon continued irradiation. The quantum yield for this transformation was measured to be approximately

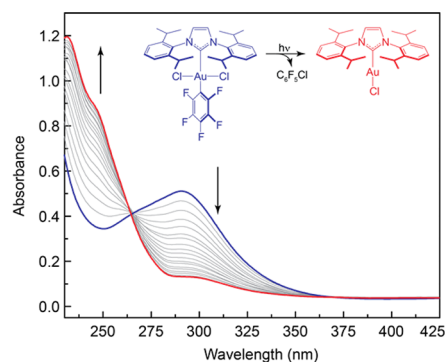


Figure 2. UV-vis time course showing the changes in the absorption profile accompanying the photoconversion ($\lambda_{\text{exc}} \geq 275$ nm) of $[(\text{IPr})\text{Au}^{\text{III}}(\text{Cl})_2\text{C}_6\text{F}_5]$ (100 μM) to $[(\text{IPr})\text{Au}^{\text{I}}\text{Cl}]$ in CH_2Cl_2 at 298 K. The reactant and product are matched by color to their respective absorption profiles. Spectra were recorded over the span of 12 h at 30 min intervals.

9% upon excitation of $[(\text{IPr})\text{Au}^{\text{III}}(\text{Cl})_2\text{C}_6\text{F}_5]$ with monochromatic light of λ_{exc} 312 nm. The course of the photoreaction was also followed by ^1H NMR spectroscopy, which confirmed the formation of $[(\text{IPr})\text{Au}^{\text{I}}\text{Cl}]$ (Figure S2, Supporting Information). Generation of $\text{C}_6\text{F}_5\text{Cl}$ as the elimination product was confirmed by a combination of ^{19}F NMR and GCMS.

Oxidation of $[(\text{IPr})\text{Au}^{\text{I}}\text{Ph}]$ with PhICl_2 proceeds in a very different manner. Addition of PhICl_2 to $[(\text{IPr})\text{Au}^{\text{I}}\text{Ph}]$ did not generate a Au^{III} complex but rather directly delivered $[(\text{IPr})\text{Au}^{\text{I}}\text{Cl}]$. Formation of this product was accompanied by production of 1 equiv of chlorobenzene, as judged by ^1H NMR and GCMS analyses. Direct formation of $[(\text{IPr})\text{Au}^{\text{I}}\text{Cl}]$ and chlorobenzene was also observed to be rapid when this reaction was carried out in the dark at temperatures as low as -33°C . This observation is consistent with initial formation of $[(\text{IPr})\text{Au}^{\text{III}}(\text{Cl})_2\text{Ph}]$ as an intermediate, which rapidly undergoes facile reductive elimination to deliver the observed products (Scheme 2). The intermediacy of this Au^{III} dichloride along the reaction pathway is akin to that which has been invoked for oxidation of homologous phosphine- and arsine-supported Au^{I} -aryl complexes with X_2 .^{25,27} Moreover, this pathway is bolstered by the isolation of $[(\text{IPr})\text{Au}^{\text{III}}(\text{Cl})_2\text{C}_6\text{F}_5]$ (vide supra) and related work by Limbach and co-workers, which demonstrated that a less sterically encumbered $\text{NHC}-\text{Au}^{\text{III}}$ complex ($[(\text{IMes})\text{Au}^{\text{III}}(\text{Cl})_2\text{Ar}]$) could be formed upon treatment of $[(\text{IMes})\text{Au}^{\text{I}}\text{Ph}]$ with PhICl_2 .²⁴ Our observation that reductive elimination from the homologous IPr-supported complex, which is more crowded around the metal center, is consistent with a reaction pathway in which ligand dissociation precedes reductive elimination.

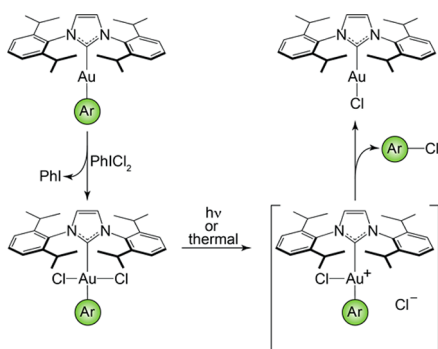
The thermal and photochemical reductive eliminations observed for the phenyl and pentafluorophenyl $\text{NHC}-\text{Au}$ complexes, respectively, may occur through similar pathways. Although the chloride and C_6F_5 groups of $[(\text{IPr})-$

Table 1. Selected Bonding Metrics for $[(\text{IPr})\text{Au}^{\text{I}}\text{Ph}]$, $[(\text{IPr})\text{Au}^{\text{I}}\text{C}_6\text{F}_5]$, and $[(\text{IPr})\text{Au}^{\text{III}}(\text{Cl})_2\text{C}_6\text{F}_5]$

	bond length (Å)				bond angle (deg)	
	Au-C(IPr)	Au-C(Ar)	Au-Cl(1)	Au-Cl(2)	C(IPr)-Au-C(Ar)	Cl(1)-Au-Cl(2)
$[(\text{IPr})\text{Au}^{\text{I}}\text{Ph}]^a$	2.0334(13)	2.0396(13)			174.44(5)	
$[(\text{IPr})\text{Au}^{\text{I}}\text{C}_6\text{F}_5]$	2.018(4)	2.021(5)			180	
$[(\text{IPr})\text{Au}^{\text{III}}(\text{Cl})_2\text{C}_6\text{F}_5]$	2.063(7)	2.049(8)	2.278(2)	2.278(2)	176.3(3)	177.36(8)

^aData reproduced from ref 21.

Scheme 2. Proposed Pathway for Reductive Elimination of Aryl Chloride from Complexes of the Type [(IPr)Au^{III}(Cl)₂Ar]



Au^{III}(Cl)₂C₆F₅] are *cis* to one another, photoexcitation likely does not induce reductive elimination directly from the four-coordinate Au^{III} center. Kochi has demonstrated that reductive elimination from square-planar Au^{III} complexes is facilitated by loss of a ligand to generate an electronically and coordinately unsaturated Au^{III} center,^{28,29} which may either adopt a T- or Y-shaped geometry.³⁰ It is this three-coordinate intermediate that ultimately undergoes elimination to generate the corresponding Au^I complex and aryl halide. Related work has shown that reductive elimination of methyl iodide from [(IPr)Au^{III}(I)₂Me] occurs via an analogous mechanism.²¹ On the basis of this mechanistic precedent, a likely pathway for the observed photoreaction involves photoinduced loss of a chloride ligand to generate [(IPr)Au^{III}(Cl)C₆F₅]Cl, which then eliminates C₆F₅Cl to give the observed Au^I product (Scheme 2).

TD-DFT conducted for [(IPr)Au^{III}(Cl)₂C₆F₅] supports this photochemical pathway. These calculations show that the main absorption (~290 nm) from which the observed photoreaction is derived involves an electronic transition resulting in excited-state population of the LUMO. This molecular orbital is comprised of antibonding interactions between d_{x²-y²} on the Au^{III} center and the ligands in the equatorial plane (Figure S3, Supporting Information). As such, photoexcitation of [(IPr)Au^{III}(Cl)₂C₆F₅] should produce an excited state in which the Au^{III}–Cl bonds are significantly weakened, which facilitates halide dissociation and subsequent reductive elimination.

A related pathway is likely operative for the thermal reductive elimination observed upon reaction of [(IPr)Au^IPh] with PhI₂. If it is presumed, on the basis of previous work involving [(IMes)Au^IPh], that [(IPr)Au^IPh] and PhI₂ initially react to form [(IPr)Au^{III}(Cl)₂Ph], the thermal dissociation of a chloride from this square-planar complex would enable reductive elimination of Ph–Cl. The observation that this process is facile for [(IPr)Au^{III}(Cl)₂Ph] but requires photoexcitation with a relatively high energy photon for [(IPr)Au^{III}(Cl)₂C₆F₅] suggests that the Au^{III}–Cl bond is stronger for the pentafluorophenyl homologue. Indeed, thermal dissociation of chloride from [(IPr)Au^{III}(Cl)₂C₆F₅] does not even occur upon treatment of this complex with AgBF₄ at 80 °C for several hours. This unusual stability is presumably due to the extent to which a C₆F₅ moiety perturbs the electron density of the Au center. This effect can be perceived by comparing the Au^{I/III} redox couples of the related Au^I–NHC complexes ([IPr)Au^IPh] and [(IPr)Au^IC₆F₅], which were measured to be 1.77 and 1.93 V versus Ag/AgCl, respectively. That the fluorinated homologue is more difficult to oxidize by

approximately 160 mV demonstrates that the gold center of [(IPr)Au^IC₆F₅] is more electron poor than that of [(IPr)Au^IPh] and highlights the ability of fluorinated aromatics to perturb the electronic structure of the gold–NHC complexes.

Electrostatic potential maps constructed for both of the [(IPr)Au^I–Ar] complexes are shown in Figure 3a. These plots

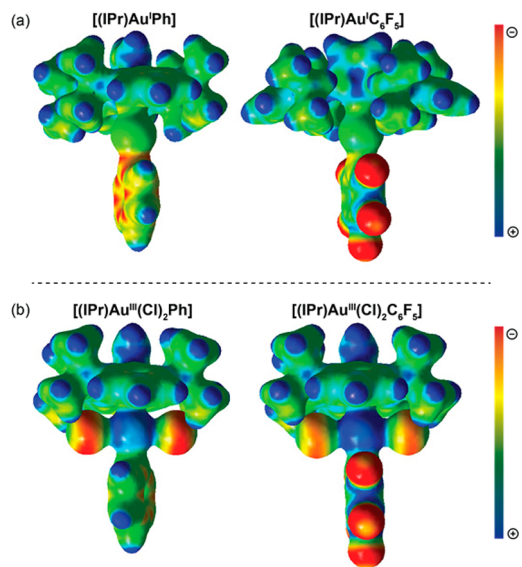


Figure 3. Electrostatic potential maps: (a) [(IPr)Au^IPh] and [(IPr)Au^IC₆F₅]; (b) [(IPr)Au^{III}(Cl)₂Ph] and [(IPr)Au^{III}(Cl)₂C₆F₅]. Each map was generated using an isovalue of 0.006 e/Å³. Red indicates areas of more negative electrostatic potential, and blue represents more positive electrostatic potential.

show that the Au^I center of the fluorinated homologue is less electron rich than the phenyl complex. This result is consistent with the difference in measured redox potentials (*vide supra*). On the basis of the ability of the fluorinated aryl ring to withdraw electron density from the metal center of [(IPr)Au^IC₆F₅], the Au^{III} center of [(IPr)Au^{III}(Cl)₂C₆F₅] should also be more electron poor than the gold atom of an [(IPr)Au^{III}(Cl)₂Ph] intermediate. Electron density maps constructed for these two systems (Figure 3b) also reveal that the metal center of the fluorinated Au^{III} complex is more electropositive than that of the phenyl-appended homologue.

The redox data together with the electrostatic potential maps provide a framework through which the divergent reactivities of [(IPr)Au^IPh] and [(IPr)Au^IC₆F₅] can be rationalized. The extent to which the pentafluorophenyl group shifts electron density away from the metal center of [(IPr)Au^{III}(Cl)₂C₆F₅] disfavors dissociation of a hard chloride anion from the electropositive Au^{III} center of this complex in comparison to the analogous process involving the more electron rich Au^{III} center of the phenyl complex. As such, a plausible explanation for the unusual stability of [(IPr)Au^{III}(Cl)₂C₆F₅] versus [(IPr)Au^{III}(Cl)₂Ph] stems from the increased electrostatic interaction between the chloride ligands and the Au^{III} center of the pentafluorophenyl complex. This electrostatic stabilization raises the barrier for halide dissociation from [(IPr)Au^{III}(Cl)₂C₆F₅], and as a result, thermal reductive elimination from this complex is not observed. In contrast, the chloride ligands should be bound much more weakly to the more electron-rich gold center of the [(IPr)Au^{III}(Cl)₂Ph] intermediate. Facile dissociation of chloride from such an

intermediate would result in the rapid reductive elimination observed for the phenyl complex.

In conclusion, we have prepared two homologous complexes of the type [(NHC)Au^I-Ar], in which the aryl substituent was either phenyl or C₆F₅. Reaction of these species with PhICl₂ proceeds differently, depending on the aryl substituent. Treatment of [(IPr)Au^IC₆F₅] with PhICl₂ leads directly to isolation of the expected Au^{III} oxidation addition product [(IPr)Au^{III}(Cl)₂C₆F₅]. This complex is thermally stable but undergoes reductive elimination upon photoexcitation to deliver [(IPr)Au^ICl] and C₆F₅Cl. In contrast, the reaction of [(IPr)Au^IPh] with PhICl₂ does not deliver an isolable Au^{III} oxidation addition product but rather leads directly to formation of [(IPr)Au^ICl] and PhCl, presumably via a [(IPr)Au^{III}(Cl)₂Ph] intermediate. Redox measurements in combination with calculated electrostatic potential maps suggest that the divergent stability of [(IPr)Au^{III}(Cl)₂C₆F₅] and [(IPr)Au^{III}(Cl)₂Ph] stems from the greater lability of the chloride ligands of the nonfluorinated Au^{III} complex, as facile dissociation of chloride from this more electron rich Au^{III} species results in rapid thermal reductive elimination. The ability of the fluorinated aromatic ring of [(IPr)Au^{III}(Cl)₂C₆F₅] to attenuate the electron density of the Au^{III} center is critical to the stability of this complex.

■ ASSOCIATED CONTENT

Supporting Information

Text, figures, tables, and CIF files giving experimental methods with accompanying crystallographic and computational data. This material is available free of charge via the Internet at <http://pubs.acs.org>.

■ AUTHOR INFORMATION

Corresponding Author

*E-mail for J.R.: joelr@udel.edu.

Notes

The authors declare no competing financial interest.

■ ACKNOWLEDGMENTS

We thank Gabriel A. Andrade (UD) for assistance with X-ray crystallography. Research reported in this publication was supported by the University of Delaware Research Foundation and the donors of the American Chemical Society's Petroleum Research Fund. M.J.G. was supported through a UD Plastino Summer Fellowship, and D.A.L. was sponsored by the Division of Chemical Sciences, Geosciences, and Biosciences, Office of BES, U.S. DOE. Data were acquired using instrumentation obtained with assistance from the NSF (CHE-0421224, CHE-0840401, CHE-1048367, and CHE-1229234). D.A.L. also thanks the Ohio Supercomputing Center.

■ REFERENCES

- (1) Mankad, N. P.; Toste, F. D. *J. Am. Chem. Soc.* **2010**, *132*, 12859–12861.
- (2) Tkatchouk, E.; Mankad, N. P.; Benitez, D.; Goddard, W. A.; Toste, F. D. *J. Am. Chem. Soc.* **2011**, *133*, 14293–14300.
- (3) Johnson, M. T.; Marthinus Janse van Rensburg, J.; Axelsson, M.; Ahlquist, M. S. G.; Wendt, O. F. *Chem. Sci.* **2011**, *2*, 2373–2377.
- (4) For an overview of the use of gold in homogeneous catalysis, please see the following and references therein: (a) Marion, N.; Nolan, S. P. *Chem. Soc. Rev.* **2008**, *37*, 1776–1782. (b) Jiménez-Núñez, E.; Echavarren, A. M. Gold in Homogeneous Catalysis. In *Nano/Microporous Materials: Mesoporous and Surface-Functionalized Meso-*
- porous Carbon*; Wiley: New York, 2005. (c) Hashmi, A. S. K. *Chem. Rev.* **2007**, *107*, 3180–3211. (d) Gorin, D. J.; Sherry, B. D.; Toste, F. D. *Chem. Rev.* **2008**, *108*, 3351–3378. (e) Li, Z.; Brouwer, C.; He, C. *Chem. Rev.* **2008**, *108*, 3239–3265. (f) Arcadi, A. *Chem. Rev.* **2008**, *108*, 3266–3325. (g) Corma, A.; Leyva-Pérez, A.; Sabater, M. J. *Chem. Rev.* **2011**, *111*, 1657–1712.
- (5) Akana, J. A.; Bhattacharyya, K. X.; Müller, P.; Sadighi, J. P. *J. Am. Chem. Soc.* **2007**, *129*, 7736–7737.
- (6) Gorske, B. C.; Mbofana, C. T.; Miller, S. J. *Org. Lett.* **2009**, *11*, 4318–4321.
- (7) Mankad, N. P.; Toste, F. D. *Chem. Sci.* **2011**, *3*, 72–76.
- (8) Hirtenlehner, C.; Krims, C.; Holbling, J.; List, M.; Zabel, M.; Fleck, M.; Berger, R. J. F.; Schoefberger, W.; Monkwius, U. *Dalton Trans.* **2011**, *40*, 9899–9910.
- (9) Teets, T. S.; Nocera, D. G. *J. Am. Chem. Soc.* **2009**, *131*, 7411–7420.
- (10) Casitas, A.; Canta, M.; Solà, M.; Costas, M.; Ribas, X. *J. Am. Chem. Soc.* **2011**, *133*, 19386–19392.
- (11) Casitas, A.; King, A. E.; Parella, T.; Costas, M.; Stahl, S. S.; Ribas, X. *Chem. Sci.* **2010**, *1*, 326–330.
- (12) Lin, B.-L.; Kang, P.; Stack, T. D. P. *Organometallics* **2010**, *29*, 3683–3685.
- (13) Roy, A. H.; Hartwig, J. F. *J. Am. Chem. Soc.* **2003**, *125*, 13944–13945.
- (14) Díez-González, S.; Nolan, S. P. *Coord. Chem. Rev.* **2007**, *251*, 874–883.
- (15) Laitar, D. S.; Müller, P.; Gray, T. G.; Sadighi, J. P. *Organometallics* **2005**, *24*, 4503–4505.
- (16) Tsui, E. Y.; Müller, P.; Sadighi, J. P. *Angew. Chem., Int. Ed.* **2008**, *120*, 9069–9072.
- (17) de Frémont, P.; Scott, N. M.; Stevens, E. D.; Nolan, S. P. *Organometallics* **2007**, *24*, 2411–2418.
- (18) Partyka, D. V.; Zeller, M.; Hunter, A. D.; Gray, T. G. *Angew. Chem., Int. Ed.* **2006**, *45*, 8188–8191.
- (19) Partyka, D. V.; Esswein, A. J.; Zeller, M.; Hunter, A. D.; Gray, T. G. *Organometallics* **2007**, *26*, 3279–3282.
- (20) Lu, P.; Boorman, T. C.; Slawin, A. M. Z.; Larrosa, I. J. *J. Am. Chem. Soc.* **2010**, *132*, 5580–5581.
- (21) Scott, V. J.; Labinger, J. A.; Bercaw, J. E. *Organometallics* **2010**, *29*, 4090–4096.
- (22) Zhao, X. -F.; Zhang, C. *Synthesis* **2007**, 551–557.
- (23) Gaillard, S.; Slawin, A. M. Z.; Bonura, A. T.; Stevens, E. D.; Nolan, S. P. *Organometallics* **2010**, *29*, 394–402.
- (24) Pažický, M.; Loos, A.; João Ferreira, M.; Serra, D.; Vinokurov, N.; Rominger, F.; Jäkel, C.; Hashmi, A. S. K.; Limbach, M. *Organometallics* **2010**, *29*, 4448–4458.
- (25) Uson, R.; Laguna, A.; Vicente, J. J. *Organomet. Chem.* **1975**, *86*, 415–421.
- (26) Vicente, J.; Bermúdez, M. D.; Chicote, M. T.; Sanchez-Santano, M. J. *J. Organomet. Chem.* **1989**, *371*, 129–135.
- (27) Aresta, M.; Vasapollo, G. *J. Organomet. Chem.* **1973**, *50*, C51–C53.
- (28) Tamaki, A.; Magennis, S. A.; Kochi, J. K. *J. Am. Chem. Soc.* **1974**, *96*, 6140–6148.
- (29) Komiyama, S.; Kochi, J. K. *J. Am. Chem. Soc.* **1976**, *98*, 7599–7607.
- (30) Komiyama, S.; Albright, T. A.; Hoffmann, R.; Kochi, J. K. *J. Am. Chem. Soc.* **1976**, *98*, 7255–7265.